Received: 9 September 2016 | Revised: 30 December 2016 | Accepted: 16 January 2017

DOI: 10.1111/vru.12504

ORIGINAL INVESTIGATION

WILEY

# Accuracy of computed tomographic arthrography for assessment of articular cartilage defects in the ovine stifle

Fanny Hontoir[1] | Peter Clegg[2] | Vincent Simon[1] | Nathalie Kirschvink[1] | Jean-Francois Nisolle[3] | Jean-Michel Vandeweerd[1]

[1]Department of Veterinary Medicine, Integrated Veterinary Research Unit-Namur Research Institute for Life Science (IVRU-NARILIS), Faculty of Sciences, University of Namur, 5000, Namur, Belgium

[2]Department of Musculoskeletal Biology, Faculty of Health and Life Sciences, University of Liverpool, Leahurst Campus, Neston, CH64 7TE, UK

[3]Hôpital Mont-Godinne, Université Catholique de Louvain, 5530, Yvoir, Belgium

**Correspondence**
Fanny Hontoir, Department of Veterinary Medicine, Integrated Veterinary Research Unit-Namur Research Institute for Life Science (IVRU-NARILIS), Faculty of Sciences, University of Namur, Rue de Bruxelles 61, 5000 Namur, Belgium.
Email: fanny.hontoir@unamur.be

## Abstract

Articular cartilage defects are one of the features of osteoarthritis in animals and humans. Early detection of cartilage defects is a challenge in clinical veterinary practice and also in translational research studies. An accurate, diagnostic imaging method would be desirable for detecting and following up lesions in specific anatomical regions of the articular surface. The current prospective experimental study aimed to describe the accuracy of computed tomographic arthrography (CTA) for detecting cartilage defects in a common animal model used for osteoarthritis research, the ovine stifle (knee, femoropatellar/femorotibial) joint. Joints in cadaver limbs ($n$ = 42) and in living animals under anesthesia ($n$ = 13) were injected with a contrast medium and imaged using a standardized CT protocol. Gross anatomy and histological assessment of specific anatomic regions were used as a gold standard for the evaluation of sensitivity, specificity, negative predictive value, and positive predictive value for CTA identification of articular cartilage defects in those regions. Pooled estimated sensitivity and specificity were 90.32% and 97.30%, respectively, in cadaver limbs, and 81.82% and 95.24%, respectively, in living animals. Pooled estimated positive predictive value and negative predictive values were 98.25% and 85.71%, respectively, in cadaver limbs, and 81.82% and 95.24%, respectively, in living animals. The delineation of cartilage surface was good for anatomical regions most frequently affected by cartilage defects in the ovine stifle: medial femoral condyle, medial tibial condyle, and patella. This study supported the use of CTA as an imaging technique for detecting and monitoring articular cartilage defects in the ovine stifle joint.

**KEYWORDS**
chondral loss, knee, scanner, sheep

## 1 | INTRODUCTION

Articular cartilage defects have been described in many species. In man, cartilage injuries of the knee (femoropatellar/femorotibial) joint are very common, particularly in young and active people, and are considered to be risk factors for the development of osteoarthritis.[1] Osteoarthritis is a degenerative and inflammatory disease of the joint, also resulting in deterioration and loss of articular cartilage matrix.[2] An estimated 60% of human patients who undergo knee arthroscopy will have shown articular cartilage defects,[3–5] even without clinical signs.[6,7] Articular cartilage defects are also prevalent in racehorses, affecting 33% of equine metacarpophalangeal joints.[8] Studies in dogs have reported articular cartilage erosions in the elbow of 30% of mature dogs (more than 6 years old),[9] and in the humeral head, in 52% of animals.[10] Subclinical articular cartilage defects have also been described in large animal models that are commonly used for osteoarthritis research, such as the ovine stifle (knee, femoropatellar/femorotibial) joint. We have previously shown fibrillation and fissures not involving the subchondral bone, as well as erosions down to subchondral bone, which were present in 43% of a population of crossbred Texel ewes used for research and were more commonly identified in specific anatomical regions such as the middle part of the medial femoral condyle, the medial tibial condyle, and the patella.[11] In some experimental studies, cartilage defects are created in specific anatomic sites to test surgical or regenerative therapies, in particular the medial femoral condyle.[12] In clinical cases, since regeneration of damaged or lost articular cartilage is currently an unachieved goal,[13] it is likely that it is useful to detect articular cartilage lesions early in the course of disease, although the clinical significance of articular cartilage defects in asymptomatic animals or patients has yet to be

  

determined. In research, the follow-up of cartilage defects, identified at baseline or surgically created in specific anatomic regions, is a useful outcome measure.

Noninvasive identification of articular cartilage defects can be performed by imaging techniques such as magnetic resonance imaging (MRI) or computed tomography arthrography (CTA) and have been well described.[14–17] In humans, CTA seems to be more accurate than MRI to detect cartilage defects.[14,16–18] An *ex vivo* study in horses demonstrated that 3T MRI using specific sequences for cartilage evaluation (dual echo in the steady state [DESS], sampling perfection with application-optimized contrast using different flip-angle evolutions [SPACE]) was less accurate than CTA to detect small naturally occurring articular cartilage defects in the metacarpo(tarso)phalangeal joints.[19]

There is need to improve techniques to assess defects noninvasively in clinical cases or in longitudinal clinical or experimental research studies.[11,20] The objectives of the current study were (1) to assess the accuracy of CTA to detect naturally occurring articular cartilage defects of the stifle (knee) joint in an *ex vivo* study on a sheep population and (2) to determine whether this technique is feasible in living animals enrolled in a research protocol.

## 2 | MATERIAL AND METHODS

### 2.1 | *Ex vivo* study

#### 2.1.1 | Animals

The experimental protocol (reference: VA10 150) was approved by the local ethics committee for animal welfare. Paired hind limbs were collected from Texel crossbred ewes (aged from 2 to 11 years) euthanized for reasons not related to musculoskeletal disease (mastitis, loss of fertility) and used for teaching (anatomical dissection). The sheep weighed between 45 and 80 kg. They came from the Ovine Research Centre of the University of Namur. Animals were euthanized by an IV injection of embutramide (20 mg/kg). The limbs were collected within 6 h of euthanasia and disarticulated at the level of the coxofemoral joint. They were stored frozen (−12°C) and thawed to room temperature before CTA assessment.

#### 2.1.2 | Study design

The study was a prospective, experimental design. Computed tomographic arthrography, macroscopic, and histologic scoring of articular surfaces were performed in 26 anatomic regions for every stifle (Fig. 1A–D). Sensitivity and specificity of CTA for detecting cartilage defects were calculated by comparison of CTA assessments of articular cartilage sites (one anatomic region in one stifle in a specific sheep was defined as one "site") to the combined gross anatomic and histological observation of those sites considered as the gold standard. This meant that only articular cartilage sites where lesions (cases) or absence of lesion (controls) were corroborated by histological assessment were used to assess sensitivity and specificity.

The anatomical site was considered the unit of observation for several reasons. First, the objective of the study was to evaluate CTA as a tool to identify defects in the anatomic sites that are either commonly affected at baseline or sampled for analysis[11] (and not the other sites), or to follow-up a lesion surgically induced in a specific anatomic site such as the medial femoral condyle that is commonly used in research on regenerative and graft therapies.[12] Then, considering the joint as the unit of observation would require assessing the whole articular surface histologically, which is not feasible technically. Finally, a previous prevalence study has shown that higher scores in one site (the axial part of the middle part of the tibial condyle, e.g.) do not necessarily imply that higher scores would also be identified in other sites of the joint (i.e., the axial part of the middle part of the femoral condyle).[11]

#### 2.1.3 | Sample size determination

The total number of sites (sample size, $N_{total}$), and the number of cases ($N_{cases}$) and controls ($N_{controls}$), that were necessary to assess to ensure the reliability of the sensitivity and specificity analysis, were calculated using the following equation:[21]

$$N_{total} = \frac{Z_{\alpha/2} \times Sen\ (1 - Sen)}{d^2 \times \text{Prev,}}$$

where $Z_{\alpha/2}$ was 1.96 for alpha = 0.05,

Sen = predetermined value of sensitivity, estimated from previous published studies (it was set to 0.80 in comparison to values for detection of cartilage defects in the human knee,[14] ankle,[22] and elbow,[23] and the equine fetlock joint,[19]

$d$ = precision of estimate, i.e. the maximum difference between estimated sensitivity (or specificity) and the true value was set to 0.10,[21]

Prev = prevalence of disease (cartilage defects for sheep) and was set to 0.66 according to published studies.[11]

With these settings, the sample size calculation was 93.1. This meant that 94 comparisons between gold standard and CTA assessment were required to ensure a reliable accuracy study for detection of cartilage defects in the ovine stifle with CTA.

$N_{cases}$ and $N_{controls}$ were calculated using the following equations:

$$N_{controls} = N_{total} \times (1 - \text{Prev})$$

$$N_{cases} = N_{total} \times \text{Prev.}$$

A total 62 cases were therefore required and 32 controls were necessary. These were randomly selected in the cadaveric limbs. Sheep were enrolled until those numbers were achieved. Paired hind limbs ($n$ = 42) from 21 ewes were collected to reach the adequate sample size of "sites."

#### 2.1.4 | Computed tomographic angiography technique

A 6-ml volume of ionic contrast material (iodine 320 mg/ml, at 37°C; meglumine ioxaglate and sodium ioxaglate; Hexabrix 320, Guerbet, Aulnay-Sous-Bois, France) mixed with 14 mL saline was injected through a 21G 1 $^{1/2}$ needle (Terumo, Belgium) placed in the femoropatellar compartment of the stifle. A paraligamentous technique was used: the needle was inserted along the medial aspect of the patellar ligament at mid-distance between its distal and proximal

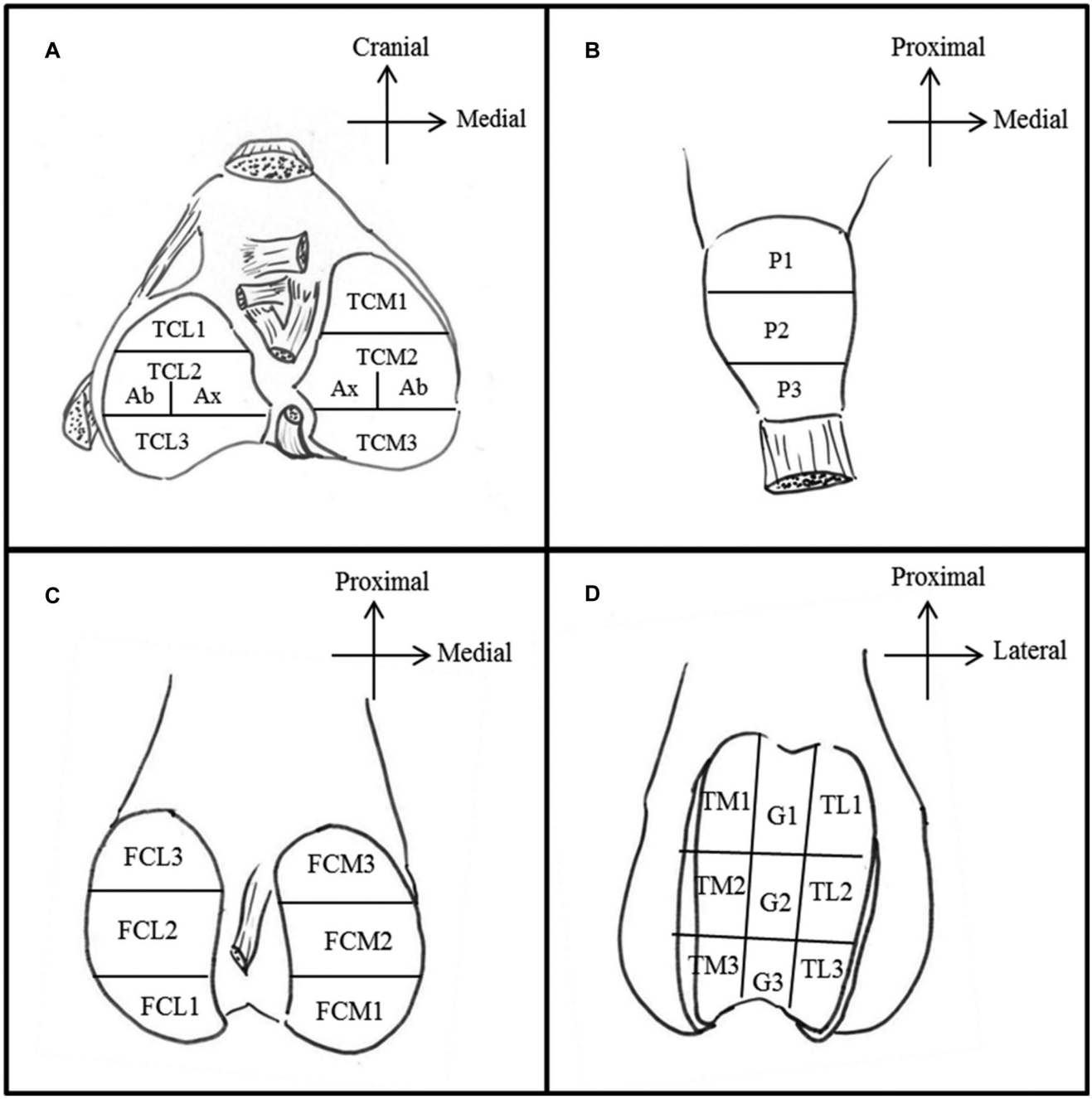


**FIGURE 1** Twenty-six anatomic subregions assessed for abnormalities of the articular cartilage. (A) cranial, middle, and caudal thirds of the articular surface of the medial and lateral tibial condyles, where each middle third was divided into axial and abaxial aspects (TCM1, TCM2Ax, TCM2Ab, TCM3, TCL1, TCL2Ax, TCL2Ab, TCL3); (B) proximal, middle, and distal thirds of the articular surface of the patella (P1, P2, P3); (C) cranial, middle, and caudal thirds of the articular surface of the medial and lateral femoral condyles (FCM1, FCM2, FCM3, FCL1, FCL2, FCL3); (D) proximal, middle, and distal thirds of the articular surface of the medial ridge, groove, and lateral ridge of the trochlea of the femur (TM1, TM2, TM3, G1, G2, G3, TL1, TL2, TL3).

insertions.[24] The injected stifles were then flexed and extended 100 times to allow homogeneous coating of the articular surfaces.

The limbs were examined with a multislice CT scanner (Emotion 6, 6-slice detector, Siemens, Erlangen, Germany). The image acquisition protocol was as follows: 130 kV, 140 mAs, pitch 0.4 (helical acquisition), collimation 0.63 mm, and tube rotation time 0.6 s. Images of 0.63 mm were reconstructed with an increment of 0.3 mm. From this isotropic volume of images, dorsal (coronal), sagittal, and transverse planar reformatted images were generated (1 mm thickness and 1 mm space between slices). The field of view extended from the base of the patella to 6 cm distal to the tibial plateau. Images were reconstructed on a 512-512 matrix, and in-plane resolution was 0.2 mm. Acquisition time was 2 min on average. The dose-length product, reflecting the radiation output from the CT scan and its extent,[25] was 143 mGray·cm. Images were then transferred on a medical digital imaging system (PACS, Télémis, Louvain-La-Neuve, Belgium).

All reconstructed images were prospectively stored for assessment of cartilage. Images were reconstructed using bone algorithm (B70, Siemens). The window center and width were 800 HU and 2000 HU, respectively.

#### 2.1.5 | Macroscopic assessment of articular cartilage

Soft tissue was removed from the detached limbs and the joint was carefully disarticulated. The cartilage was kept moist by covering the joint surface with gauze sponges soaked in lactated Ringer's solution. The distal articular surface of the femur, proximal articular surface of the tibia, and articular surface of the patella were examined by gross observation by one investigator (FH). Joint surfaces were digitally photographed (Sony Alpha DSLR-A230 digital camera) with standardized lighting conditions for records (two Sony Illustar SM-300 lighting). The abnormalities of the articular cartilage were scored by using Osteoarthritis Research Society International (OARSI) recommendations for macroscopic scoring of cartilage in sheep: score 0 for intact cartilage surface; score 1 for surface roughening; score 2 for deeper defects (fibrillation, fissures) not involving the subchondral bone; score 3 for erosions down to subchondral bone, smaller than 5 mm in diameter; score 4 for erosions down to subchondral bone, larger than 5 mm diameter.[26]

#### 2.1.6 | Microscopic assessment of articular cartilage

Sets of 3- to 4-mm-thick osteochondral slabs were obtained centered either on the articular surface defect visualized grossly, or on the center of healthy anatomic regions. Samples were fixed in 10% (v/v) neutral buffered formalin for 48 h. Following fixation, samples were transferred to 70% (v/v) ethanol for storage or further processing. They were decalcified in DC3 (nonionic surfactants, hydrochloric acid, EDTA, VWR International, Leuven, Belgium) for 2 days and embedded in paraffin, and then 4-$\mu$ sections were cut. Sections were deparaffinized with xylene and graded ethanol, and then stained with toluidine blue. Each slice was examined by two investigators (FH, JMV) working in consensus and cartilage structure was scored using the OARSI recommendations for histological evaluation of articular cartilage in sheep (Table 1).[26]

**TABLE 1** Osteoarthritis research society international (OARSI) recommendations for histological assessment of cartilage structure[26]

| Score | Definition |
|---|---|
| 0 | Normal |
| 1 | Slight surface irregularities (surface barely disturbed) |
| 2 | Moderate surface irregularities (surface roughened) |
| 3 | Severe surface irregularities (disruption, fissuring/fibrillation to <10% depth) |
| 4 | Fissures to transitional zone (1/3 depth) |
| 5 | Fissures to radial zone (2/3 depth) |
| 6 | Fissures to calcified zone (full depth) |
| 7 | Erosion or severe fibrillation to mid-zone (1/3 depth) |
| 8 | Erosion or severe fibrillation to deep zone (2/3 depth) |
| 9 | Erosion or severe fibrillation to calcified zone (full depth) |
| 10 | Erosion or severe fibrillation to subchondral bone |

### 2.2 | *In vivo* study

#### 2.2.1 | Animals

All procedures complied with the Royal Decree on the Protection of Experimental Animals in concordance with European Directive 2010/73. Thirteen unpaired hind limbs ($n = 13$) from 13 other animals (aged from 2 to 11 years), enrolled in a research study on osteoarthritis (experimental protocol OsteoOvin KI 12 181 approved by the local ethical committee for animal welfare), were used to assess the technique in living animals under general anesthesia. After the procedure, they were euthanized and limbs were collected. The sheep weighed between 45 and 80 kg. They came from the Ovine Research Centre of the University of Namur.

#### 2.2.2 | Anesthesia technique

In living animals, physical examination was performed to confirm their good health. Animals were fasted for 12 h, with ad-lib access to water. Before anesthesia, forearms were clipped and the right cephalic vein was catheterized with a 20 G 1 ¼″ catheter (Terumo). Xylazine (150 $\mu$g / kg IV) and diazepam (150 $\mu$g /kg IV) were used for premedication.[27] After induction with pentobarbital (3 mg/kg), the animal was initially placed in sternal position and the neck was extended. A laryngoscope (Kawe, Germany) was used to visualize the glottis, and a cuffed 8.0 endotracheal tube was inserted, inflated with 15 ml air, and secured. It was connected to an ambu-bag and 100% oxygen was administered. Anesthesia was maintained by IV infusion of pentobarbital in 0.9% NaCl (10 mg/kg/h).

#### 2.2.3 | Computed tomographic arthrography technique

Animals were placed in lateral recumbency and the stifle region was clipped and scrubbed with povidone iodine (Poviderm scrub, povidone iodinum 7.5%, Audevard, France; Poviderm dermicum, povidone iodinum 10%, Ecuphar, Belgium). The stifle was injected with the same technique as for the cadaver limbs. When the needle was inserted, synovial fluid was collected to confirm intra-articular position of the needle.

Animals were kept in lateral recumbency during the scanning period, with the head in a lowered position in a styrofoam box to collect saliva (Fig. 2A and B). Urinary catheterization (Foley catheter 14, Rusch Gold, Germany; connected to a 2.0L-secretion bag, Sarstedt, Germany) was performed to ensure collection of urine and to avoid contamination of the equipment and environment. Digital extremities were covered with latex gloves. To perform CT scan, the targeted limb was extended caudally and maintained with a 5 kg load, while the other limb was extended cranially and maintained with a roller bandage (Fig. 2C). The limbs were examined with the same scanner as that used for the *ex vivo* study (Emotion 6, 6-slice detector, Siemens). The acquisition protocol was also similar to the *ex vivo* study except that scans were performed at 200 mAs. The dose-length product was 258 mGray·cm. The duration of the whole procedure (anesthesia and CTA) was measured.

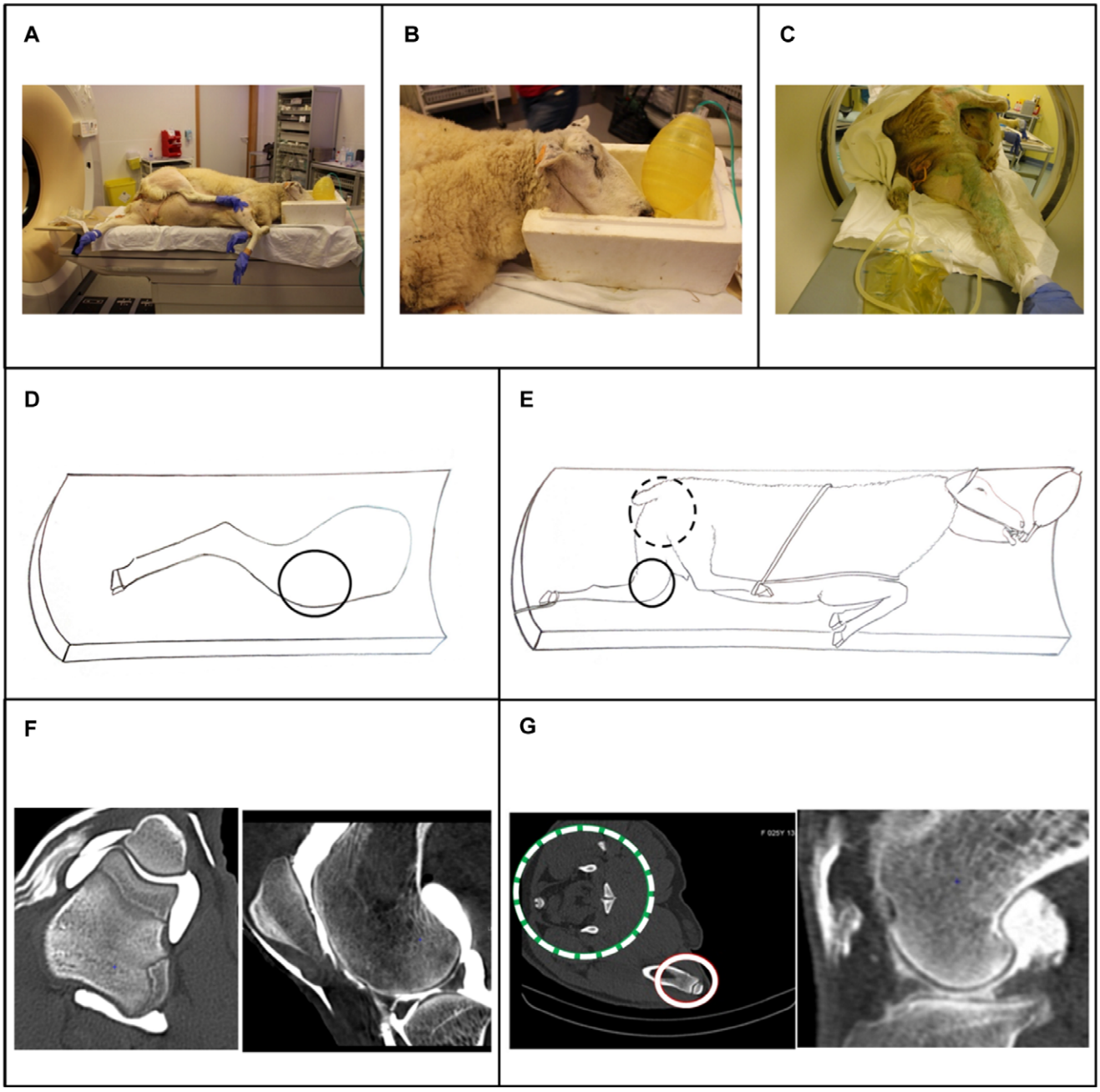


**FIGURE 2** Sheep positioning for computed tomography arthrography procedure. (A) The sheep was placed in lateral recumbence with the targeted limb extended caudally and the contralateral limb pulled cranially and tied around the trunk with a roller bandage. Digital extremities were covered with latex gloves. (B) Oxygen supply was provided by an endotracheal tube connected to an ambu-bag (VTrade, Noville-Les-Bois, Belgium) and an oxygen tank. Saliva was collected in a stir foam box. (C) Urine was collected by bladder catheterization to avoid contamination of the equipment and environment. (D) Schematic view of limb positioning for a cadaver stifle and (E) for living animal. In living animal, despite the forced extension of the limb, the pelvis remained in the acquisition field; this affected the quality of the image since the pelvis (dotted circle), soft tissues, and stifle (plain circle) attenuated the X-rays before they reached the detectors. (F) CTA images of cadaver stifle and (G) stifle of living animal. [Color figure can be viewed at wileyonlinelibrary.com]

### 2.2.4 | Macroscopic and microscopic assessment of articular cartilage

After imaging, animals were euthanized by an IV injection of embutramide (20 mg/kg). The limbs were collected within 6 h of euthanasia and disarticulated at the level of the coxofemoral joint. Soft tissue was removed from the detached limbs, and the joint was carefully disarticulated. The experimental protocol for living sheep included systematic assessment of five anatomic regions in every limb: middle third of the articular surface of the medial and lateral femoral condyles, middle third of the articular surface of the patella, axial aspect of the middle third of the articular surface of the medial and lateral tibial condyles. Gross anatomy and histology were

performed as in the in vitro study using the previously described scoring protocol.

## 2.3 | Data analyses

### 2.3.1 | Image analysis

Two months after performing CTA, one musculoskeletal radiologist (JFN) and one veterinarian (FH) separately retrieved and analyzed the archived CTA images. Transverse, dorsal, and sagittal images were viewed simultaneously. Both observers were blinded to the identity of the specimens. The 26 anatomic regions (Fig. 1A–D) were observed in each stifle. The CTA scoring criteria are described in Table 2. Normal cartilage was defined as a radiolucent layer covering the high attenuating subchondral bone and bordered by the radiopaque contrast medium. Lesions associated with osteoarthritis (osteophytes, subchondral bone changes) were also recorded as present or absent. Scores from 0 to 4 were used for CTA and corresponded to the scores used for macroscopic examinations. When surface scoring differed between the imaging planes of CT, the most severe score was reported. The most severe lesion observed in any section of each of the 26 anatomic regions was used to score the articular cartilage surface of that region. After a 1-month delay, one investigator (JFN) repeated the blinded retrospective interpretation of all examinations to determine intraobserver reproducibility.

### 2.3.2 | Statistical analysis

The prevalence (number of defects/number of observed limbs) and anatomical distribution of (number of defects per region/total number of lesions) of defects were assessed both for cadaver limbs and limbs from living sheep. Statistical analyses were performed by the first author (FH) using a computer software system (Stats Direct, Medical Statistics Software, Cheshire, UK). Kolmogorov–Smirnov and Shapiro–Wilk tests were used to examine the normality of data. Due to positive skewness and kurtosis of the macroscopic, histologic and imaging scores distribution, nonparametric statistics were conducted.[28] According to the requirements of the sensitivity–specificity analysis, data were used for analysis only if macroscopic scores were confirmed by histology; this means that macroscopic scores of 1, 2, 3, and 4 corresponded, respectively, to histological (1) surface irregularities from moderate to severe but where disruption, fissuring, and fibrillation do not reach more than 10% of articular cartilage depth (OARSI scores 2 and 3; Table 1); (2) fissures, erosions, or fibrillations that do not go deeper than the calcified layer (OARSI scores 4–9; Table 1); (3 and 4) erosion or severe fibrillation to subchondral bone (OARSI score 10; Table 1). Using the Spearman rank coefficient assessed correlation between macroscopic scoring and histological scoring. Interobserver and intraobserver agreement were tested by using Kappa statistics. Kappa values less than 0 were considered to be poor agreement; between 0 and 0.2, slight agreement; between 0.21 and 0.40, fair agreement; between 0.41 and 0.60, moderate agreement; between 0.61 and 0.80, substantial agreement; and between 0.81 and 1.00, almost perfect agreement.[29] Sensitivity, specificity, positive predictive value, and negative predictive value were calculated separately for cadaver limbs and living animals. Pooled estimated sensitivity, specificity, positive predictive value, and negative predictive value were calculated after consensus between observers was reached. Pooled estimated parameters for cadaver limbs and living animals were then compared using chi-square test (and Fischer's exact test when required). A $P$-value $< 0.05$ was considered to indicate a statistically significant difference.

# 3 | RESULTS

## 3.1 | Descriptive statistics

The CTA duration was 2 min. The whole procedure (anesthesia and CTA) had a mean duration of 40 min. No complications occurred in the living animals. A total of 115 osteochondral samples were assessed, including 99 that had their macroscopic scoring confirmed by histology and were used for sensitivity–specificity analysis. Prevalence and anatomical distribution are described in the flow chart in Fig. 3. Lesions were primarily score-2 defects (71.0%). Score-1 defects, score-3 defects, and score-4 defects accounted for 24.2%, 1.6%, and 3.2%, respectively. Most frequent affected anatomic regions were: middle third of the articular surface of the medial tibial condyle) (50.0%) and middle third of the articular surface of the medial femoral condyle (27.4%). No signs of osteoarthritis (such as osteophytes and subchondral bone changes) were identified by CTA either in the cadaver limbs or in living animals. Figure 4 illustrates the appearance of articular cartilage at CTA and examples of scores 2 and 3 defects.

## 3.2 | Sensitivity/specificity analysis

Including all slides (even those where histological scores were not similar to macroscopic scores), gross anatomy findings

**TABLE 2** Macroscopic and computed tomographic arthrography scoring scales

| Score | Macroscopic scoring | CTA scoring |
|---|---|---|
| Score 0 | Intact cartilage surface | A sharp line of contrast material is identified on the cartilage surface without substance loss |
| Score 1 | Surface roughening | Loss of the sharp and smooth contour of the cartilage surface |
| Score 2 | Deeper defects (fibrillation, fissures) not involving the SB | Penetration of contrast material within at least the superficial half of the cartilage thickness but not down to the SB |
| Score 3 | Erosion down to SB, <5 mm diameter | Penetration of contrast material down to SB, <5 mm diameter |
| Score 4 | Erosion down to SB, >5 mm diameter | Penetration of contrast material down to SB, >5 mm diameter |

SB, subchondral bone; CTA, computed tomographic arthrography; mm = millimeter.

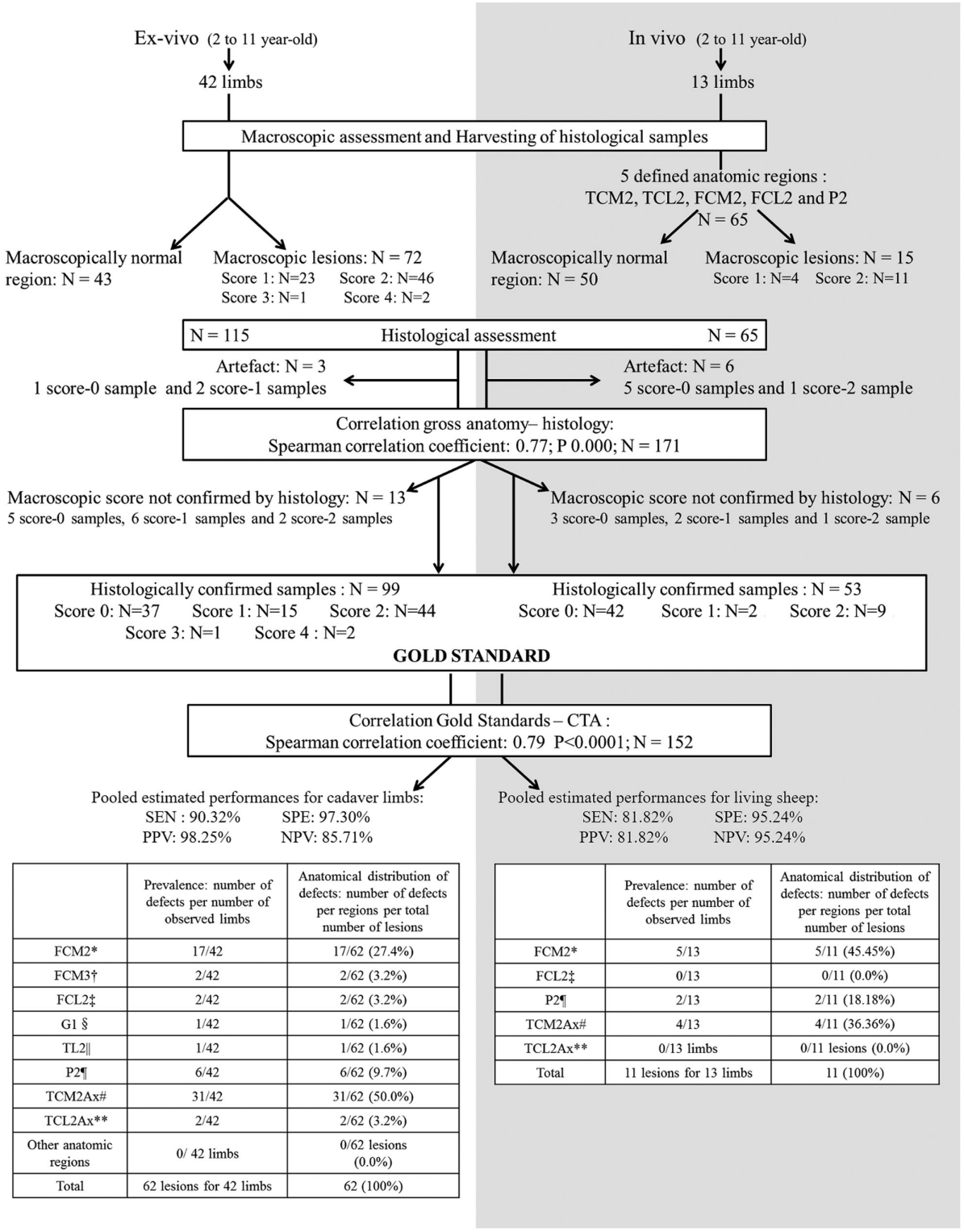


| | Prevalence: number of defects per number of observed limbs | Anatomical distribution of defects: number of defects per regions per total number of lesions |
|---|---|---|
| FCM2* | 17/42 | 17/62 (27.4%) |
| FCM3† | 2/42 | 2/62 (3.2%) |
| FCL2‡ | 2/42 | 2/62 (3.2%) |
| G1 § | 1/42 | 1/62 (1.6%) |
| TL2‖ | 1/42 | 1/62 (1.6%) |
| P2¶ | 6/42 | 6/62 (9.7%) |
| TCM2Ax# | 31/42 | 31/62 (50.0%) |
| TCL2Ax** | 2/42 | 2/62 (3.2%) |
| Other anatomic regions | 0/ 42 limbs | 0/62 lesions (0.0%) |
| Total | 62 lesions for 42 limbs | 62 (100%) |

| | Prevalence: number of defects per number of observed limbs | Anatomical distribution of defects: number of defects per regions per total number of lesions |
|---|---|---|
| FCM2* | 5/13 | 5/11 (45.45%) |
| FCL2‡ | 0/13 | 0/11 (0.0%) |
| P2¶ | 2/13 | 2/11 (18.18%) |
| TCM2Ax# | 4/13 | 4/11 (36.36%) |
| TCL2Ax** | 0/13 limbs | 0/11 lesions (0.0%) |
| Total | 11 lesions for 13 limbs | 11 (100%) |

**FIGURE 3** Flow chart of limbs and samples, mean performances of CTA, distribution of lesions, and prevalence of lesions for cadaver limbs and limbs from living sheep.

*FCM2: middle third of the articular surface of the medial femoral condyle

†FCM3: caudal third of the articular surface of the medial femoral condyle.

‡FCL2: middle third of the articular surface of the lateral femoral condyle.

§G1: proximal third of the articular surface of the groove of the trochlea of the femur.

‖TL2: middle third of the articular surface of the lateral femoral trochlear ridge.

¶P2: middle third of the articular surface of the patella.

#TCM2Ax: axial aspect of the middle third of the articular surface of the medial tibial condyle.

**TCL2Ax: axial aspect of the middle third of the articular surface of the lateral tibial condyle.

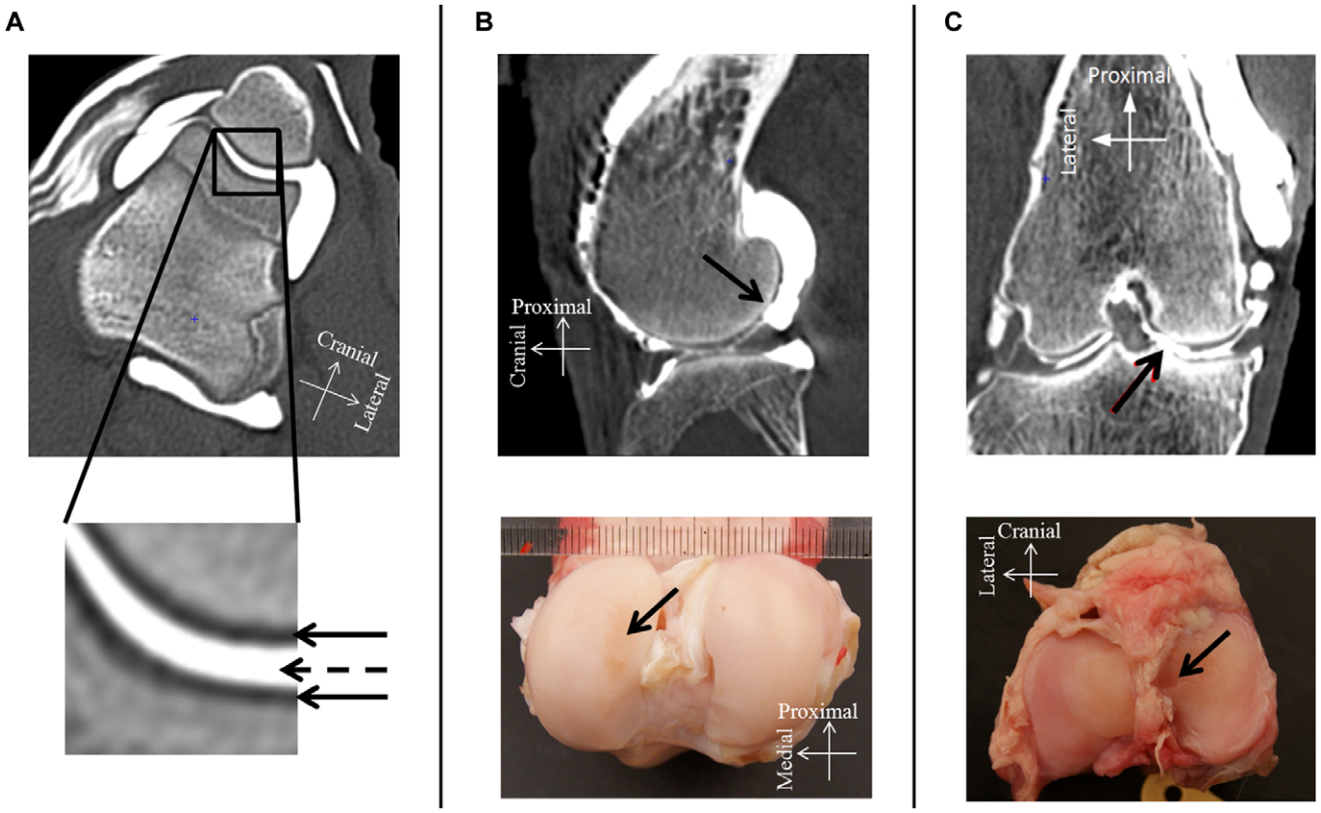


**FIGURE 4** Appearance of cartilage in CTA images. (A) Intact cartilage appears as a sharp radiolucent layer (plain arrows) underlined by the radiopaque contrast medium (dotted arrow). (B and C) Examples of cartilage defects. (B) A score-2 defect on the medial femoral condyle; (C) a score-3 defect on the axial aspect of the medial tibial condyle. [Color figure can be viewed at wileyonlinelibrary.com]

were significantly correlated with histology (Spearman correlation coefficient 0.77; $P = 0.000$). Considering only sites where macroscopic scores were corroborated by histology, there was substantial agreement between those scores and those at CTA (Spearman correlation coefficient: 0.76 (observer 1 – assessment 1), 0.81 (observer 1 – assessment 2), 0.79 (observer 2); $P < 0.0001$).

The sensitivity, specificity, positive predictive value, and negative predictive value of CTA for detecting cartilage defects are reported in Table 3, both for observers 1 and 2. In cadaver limbs, CTA was able to adequately classify on average (pooled estimated of the three assessments) 36 of 37 score-0 area, 14 of 15 score-1 defects, 39 of 44 score-2 defects, 1 of 1 score-3 defects, and 2 of 2 score-4 defects. In living animals, CTA was able to adequately classify on average (pooled estimated of the three assessment) 43 of 45 score-0 areas, 1 of 2 score-1 defects, 8 of 9 score-2 defects. The *k*-values observed for inter- and intraobserver reproducibility were 0.76 and 0.94, respectively. The negative predictive value of CTA for detecting defects in cadaver limbs was significantly lower than the negative predictive value in living animals, while the positive predictive value in cadaver limbs was significantly higher than the positive predictive value in living animals ($P < 0.05$). The sensitivity and specificity of CTA for detecting defects in living animals did not significantly differ from values in cadaver limbs.

## 4 | DISCUSSION

This study demonstrated that CTA can detect articular cartilage in cadaver sheep stifle joints with acceptable sensitivity (90%) and specificity (97%). This technique is also feasible in living sheep with acceptable sensitivity (82%) and specificity (95%). The study also showed that naturally occurring articular cartilage defects were highly prevalent in this population of sheep, with 73 lesions being identified in 55 cadaver limbs. The most frequent locations of lesions were the axial aspect of the middle third of the articular surface of the medial tibial condyle, the middle third of the articular surface of the medial femoral condyle, and the middle third of the articular surface of the patella. This is in accordance with a previous study by the authors that demonstrated that these three regions were the most frequent affected anatomic regions.[11] In ovines, as well as in humans, the medial femorotibial compartment shows higher prevalence of cartilage defects[11] and bears a larger part of the total load than the lateral compartment.[30] In man, medial femoral condyle and patellar defects are more prevalent than lateral femoral condyle defects or trochlear defects.[4,6] The higher prevalence of defects in the medial compartment may be associated to the asymmetry of forces distribution in the stifle.[31,32]

The current study confirmed that cartilage defects can be present in a population of research sheep without clinical signs and radiographic

**TABLE 3** Performance parameters of computed tomography arthrography to detect cartilage defects

| | Cadaver limbs (*N* = 99 histological samples)[a] Estimate in percentage (95% confidence interval) | Living sheep under anesthesia (N = 53 histological samples)[b] Estimate in percentage (95% confidence interval) |
|---|---|---|
| SEN[c] | | |
| Observer 1/ assessment 1[h] | 80.65 | 81.82 |
| | (69.1–88.6) | (52.3–94.9) |
| Observer 1/ assessment 2[h] | 87.80 | 88.89 |
| | (74.5–94.7) | (56.5–98.0) |
| Observer 2 | 79.03 | 81.82 |
| | (67.4–87.3) | (52.3–94.9) |
| **Pooled estimated SEN** | **90.32** | **81.82** |
| | **(80.2–95.4)** | **(52.3–94.9)** |
| SPE[e] | | |
| Observer 1/ assessment 1[h] | 97.30 | 92.86 |
| | (86.2–99.5) | (81.0–97.5) |
| Observer 1/ assessment 2[h] | 93.75 | 100.00 |
| | (71.7–98.9) | (71.0–100.0) |
| Observer 2 | 97.30 | 95.24 |
| | (86.2–99.5) | (84.2–98.7) |
| **Pooled estimated SPE** | **97.30** | **95.24** |
| PPV[f] | **(86.5–99.5)** | **(84.2–98.7)** |
| Observer 1/ assessment 1[h] | 98.04 | 75.00 |
| | (89.7–99.7) | (46.8–91.1) |
| Observer 1/ assessment 2[h] | 97.30 | 100.00 |
| | (86.2–99.5) | (66.2–100.0) |
| Observer 2 | 98.00 | 81.82 |
| | (89.5–99.6) | (52.3–94.9) |
| **Pooled estimated PPV** | **98.25** | **81.82** |
| | **(90.6–99.7)** | **(52.3–94.9)** |
| NPV[g] | | |
| Observer 1/ assessment 1[h] | 75.00[d] | 95.12[d] |
| | (61.2–85.1) | (83.9 to 98.7) |
| Observer 1/ assessment 2[h] | 75.00[d] | 90.91[d] |
| | (53.1–88.8) | (62.3–98.4) |
| Observer 2 | 73.47[d] | 95.24[d] |
| | (59.7–83.8) | (84.2–98.7) |
| **Pooled estimated NPV** | 85.71[d] | 95.24[d] |
| | **(72.7–93.4)** | **(84.2–98.7)** |

*Notes*. Pooled estimated values (SEN, SPE, PPV, NPV) are highlighted in bold letter to distinguish them from the assessments of observer 1 and 2.

[a]From these 99 histological samples, 37 were control samples and 62 were case samples.

[b]From these 53 histological samples, 42 were control samples and 11 were case samples.

[c]Sensitivity (SEN) measures the proportion of positives (macroscopically eroded cartilage) that are correctly identified as such. Sen = TP / (TP + FN). TP = true positive; TN = true negative; FP = false positive; FN = false negative.

[d]Significantly different ($P < 0.05$).

[e]Specificity (SPE) measures the proportion of negatives (macroscopic score 0) that are correctly identified by the imaging technique. SPE = TN / (TN + FP).

[f]Positive predictive value (PPV) is the probability that a positive result at CTA (score 1, 2, or 3 defect) is truly a defect. PPV = TP / (TP + FP).

[g]Negative predictive value (NPV) is the probability that a negative result at CTA (score 0) is truly erosion-free. NPV = TN / (TN + FN).

[h]The two observers (Observer 1 and Observer 2) separately analyzed the CT images. After a 1-month delay, Observer 1 repeated the blinded retrospective interpretation (Observer 1/ assessment 2) to determine intraobserver reproducibility.

changes associated with osteoarthritis. This is important since animal studies rarely assess cartilage at baseline in clinical trials.[20] At best, radiography is used to confirm the initial healthiness of joints,[33,34] though it is known that radiographic assessment has methodological flaws and may not accurately identify cartilage changes associated with osteoarthritis.[35] Biopsy is not used to assess histological characteristics and biochemical contents of cartilage since it would create defects in articular cartilage. Therefore, caution should be used when generalizing conclusions on the basis of those experimental outcomes, and CTA might be a useful technique to detect articular cartilage defects present at baseline. Of course, compositional imaging[19] and synovial biomarkers are also useful techniques to assess the joint noninvasively,[36–38] but both are still not widely used in the sheep and need to be validated.[39–42] Detection of cartilage defects of various depths may be also useful for clinical cases. Though the size of the defect does not correlate with clinical signs,[43,44] early detection allows selection of more appropriate treatments to help limit early pathological changes in the joints.[45,46]

The good performance of CTA in the current study was expected since it is known to be a useful technique to define the cartilage surface. With CTA, the entire articular surface can be assessed in multiple planes because of the isotropic reconstruction of the joint and the delineation of the cartilage defects by the contrast medium.[47,48] In the human knee, e.g., CTA revealed articular cartilage defects in radiographically healthy joints and articular cartilage defects that were not identified by MRI.[14,49] In one of these studies, CTA accuracy was higher for the detection of knee cartilage defects (with sensitivity ranging from 80% to 94% and specificity ranging from 86% to 94%) than MRI.[14] In another human study, CTA was more accurate to detect cartilage loss even in comparison to MR arthrography.[50] In the horse, MRI was significantly less sensitive and less specific than CTA to identify articular cartilage defects in the metacarpo(tarso) phalangeal joint, even with specific sequences and a high-field magnet (3-T).[19] The high accuracy of CTA is related to the resolution and short acquisition time. Short acquisition time limits the risk of motion artefacts.[51] For example, to assess the articular cartilage in the equine metacarpo(tarso) phalangeal joint, several cartilage-specific MRI sequences (DESS, SPACE) of 5–8 min were necessary in comparison to a single 2 min acquisition with CTA.[19] Resolution is also a concern when imaging such thin structures as cartilage. Cartilage thickness of the stifle in sheep ranges from 0.3 mm to 1.23 mm ± 0.29 depending on the anatomical region.[52,53] If the voxel size is not small enough (i.e., 2 mm) and encompasses the signal of tissues with different attenuation coefficients (i.e., subchondral bone and/or contrast medium), partial volume averaging occurs and the cartilage delineation is indistinct, leading to a misinterpretation of the CT images.[54] In our study, the voxel size was 0.2 mm; this allowed accurate imaging of the sheep cartilage limiting the partial volume averaging and related misinterpretation.

In CTA, the cartilage is delineated by the contrast medium. It is therefore essential that this contrast medium reaches all parts of the synovial cavity. In the human knee and the ovine stifle, the meniscus, covering the tibial plateau and partially covering the femoral condyles, could prevent contrast to fully outline the cartilage. Passive mobilization of the joint and warming of the contrast medium (to enhance fluidity) are helpful to avoid this issue.[55–57]

Interestingly, in the current study, CTA could be performed in a short time (2 min). Total acquisition time for one limb in a living sheep was longer because it included the following multiple steps: handling the sheep, catheterization of cephalic vein, IV induction of anesthesia, intubation, urethral catheterization, positioning the sheep on the table and the limb on the gantry, scrubbing, injection of contrast medium, passive motion of the limb, and scanning the limb. All these steps took about 40 min. Lateral recumbency was preferred during scanning as it allowed the stifle to be in the center of the gantry. This is important since CT, unlike MRI, is prone to cone beam artifact, which is a deformation artifact due to the cone shape of the X-ray beam. This artifact is more important for outer detectors. Therefore the further the imaged structure is from the center of the gantry, the more important the artifact becomes.[54] Moreover, miscentering of the targeted structure is known to negatively affect the signal-to-noise ratio and to induce an increase in patient radiation dose to achieve the same image quality.[25,58,59] Though sternal recumbency is recommended in sheep and other ruminants for maximizing anesthesia safety, minimizing rumen bloating, and maximizing cardiovascular stability,[60] those problems were not seen with the lateral recumbency used in our study.

Another important concern regarding positioning is the presence of the pelvic cavity in the gantry, together with the stifle, even if the limb is caudally extended and maintained with a 5 kg load. This means that the X-ray beam has to penetrate the pelvis and the stifle before reaching the detectors (Fig. 2D–G). This induces signal attenuation and degrades the image quality, as it could happen when imaging a human patient with large body mass.[61] In our study, the tube current-time product was increased (200 mAs) to enhance image quality. However, this increase and enhancement is limited by the CT unit specifications and the ALARA (as low as reasonably achievable) principle, commonly observed in human medicine.[25] This may explain why, in living animals, images had more artifacts. However, the impact of these artifacts was minimal because sensitivity and specificity for detecting cartilage defects did not differ between live sheep and cadaver limbs.

The fact that positive predictive value (98%) and negative predictive value (86%) in cadaver limbs were different from positive predictive value (82%) and negative predictive value (95%) in living animals could be linked to the difference in the number of controls. Positive predictive value and negative predictive value are driven by the prevalence and its complement (1-prev), respectively.[62] For example, in living animals, there were 42 controls, which is proportionally higher than in cadaver limbs (37 samples). Negative predictive value is therefore higher for living animals than for cadaver limbs, even if both sensitivity and specificity are high.

In conclusion, this study demonstrated that detection of cartilage defects is feasible in the ovine stifle by CTA with excellent sensitivity and specificity. A high prevalence of naturally occurring cartilage defects were identified in this sample of sheep, with no clinical signs of lameness and no CTA signs of osteoarthritis. These findings supported the use of CTA for baseline screening and longitudinal assessment of cartilage in osteoarthritis research studies using sheep models. Future studies are needed to further develop and assess minimally invasive

techniques for assessing cartilage such as conventional CTA and MRI, MRI compositional imaging, and fluid biomarkers.

## LIST OF AUTHOR CONTRIBUTIONS

**Category 1**

- **(a)** Conception and Design: Hontoir F, Vandeweerd J-M, Clegg P, Nisolle J-F, Kirschvink N
- **(b)** Acquisition of Data: Hontoir F, Simon V, Nisolle J-F
- **(c)** Analysis and Interpretation of Data: Hontoir F, Nisolle J-F, Vandeweerd J-M

**Category 2**

- **(a)** Drafting the Article: Hontoir F, Vandeweerd J-M, Simon V, Nisolle J-F
- **(b)** Revising Article for Intellectual Content: Vandeweerd J-M, Clegg P, Kirschvink N

**Category 3**

- **(a)** Final approval of the completed article: Hontoir F, Clegg P, Simon V, Kirschvink N, Nisolle J-F, Vandeweerd J-M

## ACKNOWLEDGMENTS

We acknowledge the Namur Research Institue for LIfe Science (NARILIS) for their support and the technical team of Mont-Godine Hospital (Vanderstricht Renaud, Tallier Max, Delplace Quentin) for their help. We also thank Nadine Antoine and Joelle Piret for their help in the preparation of histological slices. We are thankful to Siemens Belgium for their support.

## REFERENCES

1. Schinhan M, Gruber M, Vavken P, et al. Critical-size defect induces unicompartmental osteoarthritis in a stable ovine knee. *J Orthop Res*. 2012;30:214–220.
2. Hamerman D. The biology of osteoarthritis. *N Engl J Med*. 1989;320:1322–1330.
3. Curl WW, Krome J, Gordon ES, Rushing J, Smith BP, Poehling GG. Cartilage injuries: A review of 31,516 knee arthroscopies. *Arthroscopy*. 1997;13:456–460.
4. Arøen A, Løken S, Heir S, et al. Articular cartilage lesions in 993 consecutive knee arthroscopies. *Am J Sports Med*. 2004;32:211–215.
5. Widuchowski W, Widuchowski J, Trzaska T. Articular cartilage defects: Study of 25,124 knee arthroscopies. *Knee*. 2007;14:177–182.
6. Flanigan DC, Harris JD, Trinh TQ, Siston RA, Brophy RH. Prevalence of chondral defects in athletes– knees: A systematic review. *Med Sci Sports Exerc*. 2010;42:1795–1801.
7. Solheim E, Krokeide AM, Melteig P, Larsen A, Strand T, Brittberg M. Symptoms and function in patients with articular cartilage lesions in 1,000 knee arthroscopies. *Knee Surg Sports Traumatol Arthrosc*. 2016;26:1610–1616.
8. Neundorf RH, Lowerison MB, Cruz AM, Thomason JJ, McEwen BJ, Hurtig MB. Determination of the prevalence and severity of metacarpophalangeal joint osteoarthritis in Thoroughbred racehorses via quantitative macroscopic evaluation. *Am J Vet Res*. 2010;71:1284–1293.
9. Coppieters E, Gielen I, Verhoeven G, Van Vynckt D, Van Ryssen B. Erosion of the medial compartment of the canine elbow: Occurrence, diagnosis and currently available treatment options. *Vet Comp Orthop Traumatol*. 2015;28:9–18.
10. Craig LE, Reed A. Age-associated cartilage degeneration of the canine humeral head. *Vet Pathol* 2013;50:264–268.
11. Vandeweerd JM, Hontoir F, Kirschvink N, et al. Prevalence of naturally occurring cartilage defects in the ovine knee. *Osteoarthritis Cartilage*. 2013;21:1125–1131.
12. Schinhan M, Gruber M, Vavken P, et al. Critical-size defect induces unicompartmental osteoarthritis in a stable ovine knee. *J Orthop Res*. 2012;30:214–220.
13. Saris DB, Dhert WJ, Verbout AJ. Joint homeostasis. The discrepancy between old and fresh defects in cartilage repair. *J Bone Joint Surg Br*. 2003;85:1067–1076.
14. Vande Berg BC, Lecouvet FE, Poilvache P, et al. Assessment of knee cartilage in cadavers with dual-detector spiral CT arthrography and MR imaging. *Radiology*. 2002;222:430–436.
15. McGibbon CA, Trahan CA. Measurement accuracy of focal cartilage defects from MRI and correlation of MRI graded lesions with histology: A preliminary study. *Osteoarthritis Cartilage*. 2003;11:483–493.
16. El-Khoury GY, Alliman KJ, Lundberg HJ, et al. Cartilage thickness in cadaveric ankles: Measurement with double-contrast multi-detector row CT arthrography versus MR imaging. *Radiology*. 2004;233:768–773.
17. Shahabpour M, Kichouh M, Laridon E, Gielen JL, De Mey J. The effectiveness of diagnostic imaging methods for the assessment of soft tissue and articular disorders of the shoulder and elbow. *Eur J Radiol*. 2008;65:194–200.
18. Daenen BR, Ferrara MA, Marcelis S, Dondelinger RF. Evaluation of patellar cartilage surface lesions: Comparison of CT arthrography and fat-suppressed FLASH 3D MR imaging. *Eur Radiol*. 1998;8:981–985.
19. Hontoir F, Nisolle JF, Meurisse H, et al. A comparison of 3-T magnetic resonance imaging and computed tomography arthrography to identify structural cartilage defects of the fetlock joint in the horse. *Vet J*. 2014;199:115–122.
20. Vandeweerd JM, Zhao Y, Nisolle JF, et al. Effect of corticosteroids on articular cartilage: Have animal studies said everything? *Fundam Clin Pharmacol*. 2015;29:427–438.
21. Hajian-Tilaki K. Sample size estimation in diagnostic test studies of biomedical informatics. *J Biomed Inform*. 2014;48:193–204.
22. Schmid MR, Pfirrmann CW, Hodler J, Vienne P, Zanetti M. Cartilage lesions in the ankle joint: Comparison of MR arthrography and CT arthrography. *Skeletal Radiol*. 2003;32:259–265.
23. Waldt S, Bruegel M, Ganter K, et al. Comparison of multislice CT arthrography and MR arthrography for the detection of articular cartilage lesions of the elbow. *Eur Radiol*. 2005;15:784–791.
24. Vandeweerd JM, Kirschvink N, Muylkens B, et al. A study of the anatomy and injection techniques of the ovine stifle by positive contrast arthrography, computed tomography arthrography and gross anatomical dissection. *Vet J*. 2012;193:426–432.
25. Mayo-Smith WW, Hara AK, Mahesh M, Sahani DV, Pavlicek W. How I do it: Managing radiation dose in CT. *Radiology*. 2014;273:657–672.

26. Little CB, Smith MM, Cake MA, Read RA, Murphy MJ, Barry FP. The OARSI histopathology initiative—recommendations for histological assessments of osteoarthritis in sheep and goats. *Osteoarthritis Cartilage*. 2010;18(Suppl 3):S80–S92.
27. Vandeweerd JM, Vermeylen A, Goossens M, et al. Anesthésie chez le mouton de laboratoire. *STAL*. 2014;4:15–19. French
28. Pearce GL, Frisbie DD. Statistical evaluation of biomedical studies. *Osteoarthritis Cartilage*. 2010;18(Suppl 3):S117–S122.
29. Viera AJ, Garrett JM. Understanding interobserver agreement: The Kappa statistic. *Fam Med*. 2005;37:360–363.
30. Taylor WR, Poepplau BM, Konig C, et al. The medial-lateral force distribution in the ovine stifle joint during walking. *J Orthop Res*. 2011;29:567–571.
31. Thomas RH, Resnick D, Alazraki NP, Daniel D, Greenfield R. Compartmental evaluation of osteoarthritis of the knee: A comparative study of available diagnostic modalities. *Radiology*. 1975;116:585–594.
32. Baliunas AJ, Hurwitz DE, Ryals AB, et al. Increased knee joint loads during walking are present in subjects with knee osteoarthritis. *Osteoarthritis Cartilage*. 2002;10:573–579.
33. Simmons EJ, Bertone AL, Weisbrode SE. Instability-induced osteoarthritis in the metacarpophalangeal joint of horses. *Am J Vet Res*. 1999;60:7–13.
34. Frisbie DD, Ghivizzani SC, Robbins PD, Evans CH, McIlwraith CW. Treatment of experimental equine osteoarthritis by *in vivo* delivery of the equine interleukin-1 receptor antagonist gene. *Gene Ther*. 2002;9:12–20.
35. Altman RD. Measurement of structure (disease) modification in osteoarthritis. *Osteoarthritis Cartilage*. 2004;12(Suppl A):S69–S76.
36. Frisbie DD, Al-Sobayil F, Billinghurst RC, Kawcak CE, McIlwraith CW. Changes in synovial fluid and serum biomarkers with exercise and osteoarthritis in horses. *Osteoarthritis Cartilage*. 2008;16:1196–1204.
37. McIlwraith CW. Use of synovial fluid and serum biomarkers in equine bone and joint disease: A review. *Equine Vet J*. 2005;37:473–482.
38. Lindhorst E, Vail TP, Guilak F, et al. Longitudinal characterization of synovial fluid biomarkers in the canine meniscectomy model of osteoarthritis. *J Orthop Res*. 2000;18:269–280.
39. Heard BJ, Achari Y, Chung M, Shrive NG, Frank CB. Early joint tissue changes are highly correlated with a set of inflammatory and degradative synovial biomarkers after ACL autograft and its sham surgery in an ovine model. *J Orthop Res*. 2011;29:1185–1192.
40. Friske J, Berg A, Welsch GH, Pachowsky M, Gelse K, Trattnig S. High-field high-resolution and microscopic T2-maps of a cartilage repair sheep model on a 7T human scanner: First results [Abstract]. *MAGMA*. 2012;25(Suppl 1):450–451.
41. Mickiewicz B, Heard BJ, Chau JK, et al. Metabolic profiling of synovial fluid in a unilateral ovine model of anterior cruciate ligament reconstruction of the knee suggests biomarkers for early osteoarthritis. *J Orthop Res*. 2015;33:71–77.
42. Welsch GH, Trattnig S, Friske J, Gelse K, Pachowsky ML. Biochemical cartilage properties in a sheep model—validation of zonal T2 mapping assessment [Abstract]. *Osteoarthritis Cartilage*. 2014;22(Suppl): S272–S273.
43. Heir S, Årøen A, Løken S, Sulheim S, Engebretsen L, Reinholt FP. Intraarticular location predicts cartilage filling and subchondral bone changes in a chondral defect. *Acta Orthop*. 2010;81:619–627.
44. Roemer FW, Guermazi A. Osteoarthritis year 2012 in review: Imaging. *Osteoarthritis Cartilage*. 2012;20:1440–1446.
45. Kelly BT, Potter HG, Deng XH, et al. Meniscal allograft transplantation in the sheep knee: Evaluation of chondroprotective effects. *Am J Sports Med*. 2006;34:1464–1477.
46. Park YS, Lim SW, Lee IH, Lee TJ, Kim JS, Han JS. Intra-articular injection of a nutritive mixture solution protects articular cartilage from osteoarthritic progression induced by anterior cruciate ligament transection in mature rabbits: A randomized controlled trial. *Arthritis Res Ther*. 2007;9:R8.
47. Holland P, Davies AM, Cassar-Pullicino VN. Computed tomographic arthrography in the assessment of osteochondritis dissecans of the elbow. *Clin Radiol*. 1994;49:231–235.
48. Tivers MS, Mahoney P, Corr SA. Canine stifle positive contrast computed tomography arthrography for assessment of caudal horn meniscal injury: A cadaver study. *Vet Surg*. 2008;37:269–277.
49. Vande Berg BC, Lecouvet FE, Malghem J. Frequency and topography of lesions of the femoro-tibial cartilage at spiral CT arthrography of the knee: A study in patients with normal knee radiographs and without history of trauma. *Skeletal Radiol*. 2002;31:643–649.
50. Omoumi P, Rubini A, Dubuc JE, Vande Berg BC, Lecouvet FE. Diagnostic performance of CT-arthrography and 1.5T MR-arthrography for the assessment of glenohumeral joint cartilage: A comparative study with arthroscopic correlation. *Eur Radiol*. 2015;25:961–969.
51. Gold GE, Chen CA, Koo S, Hargreaves BA, Bangerter NK. Recent advances in MRI of articular cartilage. *AJR Am J Roentgenol*. 2009;193:628–638.
52. Appleyard RC, Burkhardt D, Ghosh P, et al. Topographical analysis of the structural, biochemical and dynamic biomechanical properties of cartilage in an ovine model of osteoarthritis. *Osteoarthritis Cartilage*. 2003;11:65–77.
53. Frisbie DD, Cross MW, McIlwraith CW. A comparative study of articular cartilage thickness in the stifle of animal species used in human preclinical studies compared to articular cartilage thickness in the human knee. *Vet Comp Orthop Traumatol*. 2006;19:142–146.
54. Barrett JF, Keat N. Artifacts in CT: Recognition and avoidance. *RadioGraphics*. 2004;24:1679–1691.
55. Halsell RD. Heating contrast media: Role in contemporary angiography. *Radiology*. 1987;164:276–278.
56. Hughes PM, Bisset R. Non-ionic contrast media: A comparison of iodine delivery rates during manual injection angiography. *Brit J Radiol*. 1991;64:417–419.
57. Roth R, Akin M, Deligonul U, Kern MJ. Influence of radiographic contrast media viscosity to flow through coronary angiographic catheters. *Cathet Cardiovasc Diagn*. 1991;22:290–294.
58. Toth T, Ge Z, Daly MP. The influence of patient centering on CT dose and image noise. *Med Phys*. 2007;34:3093–3101.
59. Habibzadeh MA, Ay MR, Asl AR, Ghadiri H, Zaidi H. Impact of miscentering on patient dose and image noise in x-ray CT imaging: Phantom and clinical studies. *Phys Med*. 2012;28:191–199.
60. Taylor P. Anesthesia in sheep and goats. *In Practice*. 1991;13;31–36.
61. Yoshimura N, Sabir A, Kubo T, Lin PJ, Clouse ME, Hatabu H. Correlation between image noise and body weight in coronary CTA with 16-row MDCT. *Acad Radiol*. 2006;13:324–328.
62. Altman DG, Bland JM. Diagnostic tests 2: Predictive values. *BMJ*. 1994;309:102.

**How to cite this article:** Hontoir F, Clegg P, Simon V, Kirschvink N, Nisolle J-F, Vandeweerd J-M. Accuracy of computed tomographic arthrography for assessment of articular cartilage defects in the ovine stifle. *Vet Radiol Ultrasound*. 2017;58:512–523. https://doi.org/10.1111/vru.12504